A novel Aβ-fibrinogen interaction inhibitor rescues altered thrombosis and cognitive decline in Alzheimer's disease mice

Hyung Jin Ahn,[1] J. Fraser Glickman,[2] Ka Lai Poon,[1] Daria Zamolodchikov,[1] Odella C. Jno-Charles,[1] Erin H. Norris,[1] and Sidney Strickland[1]

[1]Laboratory of Neurobiology and Genetics and [2]High Throughput Screening Resource Center, The Rockefeller University, New York, NY 10065

Many Alzheimer's disease (AD) patients suffer from cerebrovascular abnormalities such as altered cerebral blood flow and cerebral microinfarcts. Recently, fibrinogen has been identified as a strong cerebrovascular risk factor in AD, as it specifically binds to β-amyloid (Aβ), thereby altering fibrin clot structure and delaying clot degradation. To determine if the Aβ–fibrinogen interaction could be targeted as a potential new treatment for AD, we designed a high-throughput screen and identified RU-505 as an effective inhibitor of the Aβ–fibrinogen interaction. RU-505 restored Aβ-induced altered fibrin clot formation and degradation in vitro and inhibited vessel occlusion in AD transgenic mice. Furthermore, long-term treatment of RU-505 significantly reduced vascular amyloid deposition and microgliosis in the cortex and improved cognitive impairment in mouse models of AD. Our studies suggest that inhibitors targeting the Aβ–fibrinogen interaction show promise as therapy for treating AD.

CORRESPONDENCE
Sidney Strickland:
strickland@rockefeller.edu

Abbreviations used: AD, Alzheimer's disease; BBB, blood–brain barrier; CAA, cerebral amyloid angiopathy; FP, fluorescence polarization; HTS, high-throughput screen; SPR, surface plasmon resonance; TAMRA, 5-carboxy-tetramethylrhodamine; tPA, tissue plasminogen activator.

Accumulating evidence suggests that cerebrovascular risk factors play an important role in Alzheimer's disease (AD) pathophysiology. Many AD patients suffer from altered cerebral blood flow, damaged cerebral vasculature, and increased cerebral microinfarcts (de la Torre, 2004; Brundel et al., 2012), and a majority of patients with dementia present with both AD and vascular pathologies (MRC CFAS, 2001; Viswanathan et al., 2009). Furthermore, cerebral amyloid angiopathy (CAA), which is the deposition of the β-amyloid (Aβ) peptide within cerebral blood vessels, results in degenerative vascular changes (Thal et al., 2008; Smith and Greenberg, 2009). Patients with both CAA and neurological pathology including neurofibrillary tangles and neuritic plaques have more severe cognitive impairment than patients with only AD pathology or CAA alone (Pfeifer et al., 2002), and reduction of CAA levels in AD transgenic mice leads to memory improvement (Park et al., 2013). Interestingly, the Nun Study showed that one-third of the participants who had neurological AD pathology were actually not demented at the time of death, but when AD pathology was concomitant with brain infarcts, there was a high prevalence of dementia found in participants (Snowdon et al., 1997; Mortimer, 2012). Thus, the identification of a molecular association between these vascular and neurological pathologies could aid in more efficient diagnoses and effective treatments for AD.

Recent studies have suggested that fibrinogen, a primary protein component of blood clots, serves as a molecular link between the vascular and neurological abnormalities observed in AD patients. Normally, fibrinogen is found in the blood and is excluded from the brain via the blood–brain barrier (BBB). However, it has been shown that: 1) fibrinogen is often localized to CAA in the brain's blood vessels and brain parenchyma in AD patients and in mouse models of AD (Paul et al., 2007; Ryu and McLarnon, 2009; Cortes-Canteli et al., 2010; Klohs et al., 2012); 2) fibrin deposition in the vasculature increases BBB dysfunction and neurovascular damage in AD mice (Paul et al., 2007;

The Rockefeller University Press $30.00
J. Exp. Med. 2014 Vol. 211 No. 6 1049-1062
www.jem.org/cgi/doi/10.1084/jem.20131751

The Journal of Experimental Medicine

Cortes-Canteli et al., 2010); 3) Aβ binds specifically to fibrinogen; and 4) fibrin clots formed in the presence of Aβ have an abnormal structure, making them resistant to degradation by fibrinolytic enzymes (Ahn et al., 2010; Cortes-Canteli et al., 2010). Overall, these results indicate that in the presence of Aβ, any fibrin clots formed might be more persistent and may exacerbate neurovascular damage and cognitive impairment. Therefore, molecules that block this interaction without affecting clotting in general could restore altered thrombosis and fibrinolysis and protect against vascular damage in AD patients, and could be used as therapeutic agents.

RESULTS

Hit identification and optimization using high-throughput screening

To investigate this idea, we designed a high-throughput screen (HTS) to identify small molecules that inhibit the interaction between Aβ and fibrinogen. Low molecular weight compounds were screened using fluorescence polarization (FP) and AlphaLISA assays in a complementary fashion to cross check the activity of the hit compounds and to ensure the removal of false-positive artifacts. Primarily, ∼93,000 compounds were screened using FP, which measured the changes in the anisotrophy induced by binding of a 5-carboxy-tetramethylrhodamine (TAMRA)–labeled Aβ peptide to fibrinogen (Fig. 1 A). Then, hits from FP were screened using AlphaLISA to independently confirm the activity of the inhibitors identified in the FP assay (Fig. 1 B). After both steps, we selected only drug-like compounds using Lipinski's Rule of Five, which allowed us to determine which chemical compounds have pharmacological properties that would make them likely orally active drugs in humans (Lipinski et al., 2001). We also filtered out artifactual compounds using a quenching assay, which identifies insoluble compounds, singlet oxygen quenchers, and biotin mimetics interfering with the AlphaLISA signal. We identified several candidate compounds with half-maximal inhibitions (IC_{50}) between 10 and 50 μM from the dose-response assays using both FP and AlphaLISA assays (Table 1).

To expand and improve our candidate compounds, we purchased a focused analogues compound library, based on combinatorial variations of scaffolds from the primary hit compounds. These analogues were screened at three different concentrations (5, 10, and 20 μM) using AlphaLISA. Next, we selected only drug-like compounds using Lipinski's Rule of Five and also included the quenching assay. If inhibition by quenching was >30%, the compounds were removed from further analyses because these compounds were more likely to be false positives. Finally, we screened the active nonquenching compounds in concentration-response experiments with freshly dissolved powders using both FP and AlphaLISA assays. We identified five drug-like compounds with IC_{50} < 3 μM by FP and IC_{50} < 10 μM by AlphaLISA (Fig. 1 C and Table 2).

In some cases, the maximum inhibition of several compounds in AlphaLISA was lower than that of FP. There are several possible reasons for these differences. First, some hit compounds showed negative quenching values, which increases the background AlphaLISA signal. Therefore, the actual inhibitory efficacy of these compounds could be higher than the results from dose–response experiments of AlphaLISA. In addition, avidity effects may cause higher IC_{50} values in AlphaLISA than FP. There could be multiple Aβ–fibrinogen interactions between acceptor bead and donor bead in AlphaLISA (Fig. 1 B), and therefore blocking one interaction may not reduce the signal.

Because both AlphaLISA and the FP assay are based on optical measurements, colored compounds could significantly modify the measurement through inner filter effects. Thus, we confirmed the potency of our candidates using a pull-down assay. All five compounds showed inhibitory effects, whereas RU-505 had significant inhibitory efficacy (Fig. 2 A). These combined experiments show that the compounds identified are inhibitors of the Aβ–fibrinogen interaction.

Soluble oligomeric Aβ has been hypothesized to be the primary toxic species in AD (Cleary et al., 2005). Therefore, we tested which form of Aβ, monomer or oligomer (prepared as in Stine et al. [2011]), interacts with fibrinogen and whether RU-505 can selectively inhibit the interaction of one or the other. Using the AlphaLISA assay, we found that both Aβ42 monomer and oligomer interact with fibrinogen, but the affinity of oligomer for fibrinogen binding is ∼4 times higher than that of the monomer (Fig. 2 B). RU-505 inhibits the interaction of both monomer and oligomer with fibrinogen, but has higher inhibitory efficacy against the monomer–fibrinogen interaction than the oligomer (Fig. 2 C).

Validation of hit compounds using in vitro clotting assay

Because the interaction between Aβ42 and fibrinogen induces a structurally abnormal fibrin clot and delays fibrin clot degradation during fibrinolysis (Ahn et al., 2010; Cortes-Canteli et al., 2010; Zamolodchikov and Strickland, 2012), one of the main objectives of our study was to identify compounds that restore Aβ-induced delayed fibrinolysis. When fibrinogen associates into a fibrin meshwork after cleavage by thrombin, the fine structure of this fibrin clot scatters light and the solution increases in turbidity. Thus, the kinetics of turbidity can be used as a read-out to analyze fibrin network formation and degradation. We tested whether our hits restored Aβ-induced altered thrombosis and fibrinolysis in vitro. Each hit compound (20 μM) or vehicle (0.4% DMSO) was incubated for 10 min with purified human fibrinogen and plasminogen in the presence or absence of Aβ42. Fibrin clot formation and degradation were analyzed by measuring turbidity immediately after adding thrombin and tissue plasminogen activator (tPA) to the mixture. In the presence of Aβ42, the maximum turbidity of the fibrin clot was decreased because Aβ altered fibrin clot structure and the dissolution of the fibrin clot was delayed (Fig. 2 D; red). RU-505 restored the Aβ-induced decrease in turbidity during fibrin clot formation (Fig. 2 D; green) and significantly reduced the delay in fibrin degradation in the presence of Aβ (Fig. 2 E). We also tested other hit compounds, including RU-965, using the turbidity assay, but none had significant effects (Fig. 2 F and

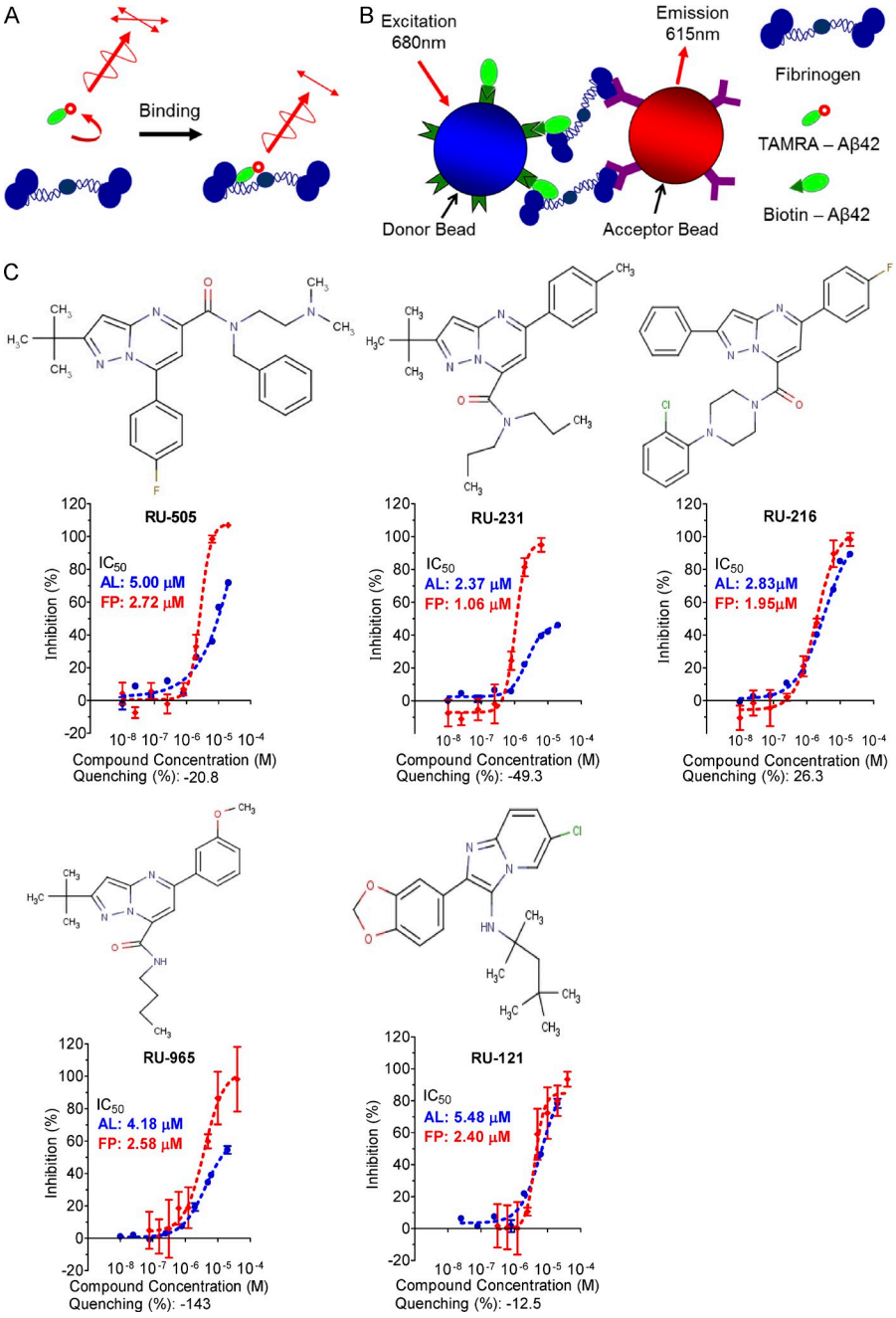

Figure 1. The chemical structure and dose–response curve of Aβ–fibrinogen interaction inhibitors. (A) TAMRA-labeled Aβ peptide was bound to fibrinogen and the test compound, and the anisotropy of TAMRA-Aβ–fibrinogen binding was determined by FP. (B) Biotin-labeled Aβ42, which binds a streptavidin donor, was incubated with fibrinogen, which binds a protein A acceptor bead coated with antifibrinogen antibody. Aβ42 and fibrinogen interactions bring the beads in close proximity, resulting in the excitation of the donor beads and release of singlet oxygen molecules that triggers light emission in acceptor beads (AlphaLISA [AL]). (C) The half-maximal inhibitory concentration (IC_{50}) values of the indicated compounds were determined by dose–response FP and AL experiments and are indicated inside the panel (red, FP; blue, AL). A quenching test was also performed to calculate how much each hit compound interfered with the AL signal at 10 μM concentration. Quenching values are indicated below the dose–response curve. n = 3–4 repeats per assay and all error bars indicate SEM. Data are representative of at least three independent experiments.

not depicted). Moreover, RU-505 did not have any effect on fibrin clot formation and degradation in the absence of Aβ (Fig. 2 D, purple). This result suggests that RU-505 could effectively restore Aβ-induced altered fibrin clot structure and delayed degradation without affecting normal clot formation and fibrinolysis.

The interaction between Aβ and RU-505

To elucidate how RU-505 inhibits the Aβ–fibrinogen interaction, surface plasmon resonance (SPR) was used to analyze the binding characteristics of RU-505 (Fig. 2 G). Hexafluoroisopropanol-treated monomerized Aβ42 was immobilized to the sensor chip surface, and RU-505 was injected for 2 min at 30 μl/min. Sulindac sulfide was used as positive control, and sulindac was used as negative control (Richter et al., 2010). To analyze the correlation between HTS and SPR, we used an analogue of RU-505, RU-4180 (Fig. 2 H), which did not inhibit the Aβ–fibrinogen interaction in AlphaLISA assay. Although RU-4180 weakly binds to Aβ42 (green; Fig. 2 G), RU-505 showed strong binding to Aβ42 (blue; Fig. 2 G). Furthermore, because it is known that sulindac sulfide binds Aβ, we tested whether it could inhibit the Aβ–fibrinogen interaction by AlphaLISA and found that it had no effect. These results suggest that RU-505 inhibits the Aβ–fibrinogen interaction

Table 1. Workflow of high-throughput primary screening

Step	Test compound concentration	Number of compounds	% of picked compounds	Inhibition cut-off (%)
Total library compound	-	93,716	-	-
Primary assay hits using FP	20 µM	3,010	3.21	>75
Secondary assay hits using AlphaLISA (AL)	12.5 µM	167	0.18	>50
Filtering using quenching (AL)	12.5 µM	97	0.1	<30
Lipinski's rule		87	0.09	≤1 violation
Validation/dose–response Hits (FP and AL)	0.31–40 µM	26	0.028	IC_{50} <50 µM
Dose–response using fresh compound (FP and AL)	0.07–40 µM	10	0.011	IC_{50} <50 µM

through Aβ binding, but RU-4180 does not inhibit the interaction because its affinity for Aβ is too weak. Moreover, from the case of sulindac sulfide, Aβ binding itself is not enough to inhibit the interaction between Aβ and fibrinogen. To inhibit the Aβ–fibrinogen interaction, a compound requires at least two features: 1) an Aβ-specific binding moiety and 2) a moiety responsible for inhibiting fibrinogen's binding to Aβ.

RU-505 restored altered thrombosis in AD mice

To assess whether our lead compound could restore Aβ-induced altered thrombosis and fibrinolysis in vivo, we examined cerebral blood flow and thrombosis in a transgenic mouse model of AD, Tg6799 mice (Oakley et al., 2006), with or without long-term treatment of RU-505. Blood flow and thrombosis were analyzed by a $FeCl_3$-induced thrombosis model combined with intravital microscopy (Cortes-Canteli et al., 2010). We administered RU-505 or vehicle (35 mg/kg dose, every other day) to 4-mo-old Tg6799 and WT littermates for 4 mo (analyzed at 8 mo of age). Brains of 8-mo-old Tg6799 or WT mice were exposed by craniotomy, and blood flow was observed using injected fluorescence-conjugated dextran (Fig. 3 A). Three concentrations of $FeCl_3$ (5, 10, and 15%) were incrementally administered to the brain surface to induce thrombosis. Clot formation was revealed by the appearance of an enlarging shadow superimposed on normal blood flow (Fig. 3 A and Videos 1–4). The length of all visible vessels with >20 µm diam was measured before $FeCl_3$ treatment, and the length of occluded vessels was measured 5 min after the addition of each concentration of $FeCl_3$ for both Tg6799 and WT. There was no significant difference in the percentage of occluded vessels before $FeCl_3$ treatment or after 5 and 10% $FeCl_3$ treatment among groups (Fig. 3 B). However, there was a significant difference between the percentage of occluded vessels after 15% $FeCl_3$ treatment in vehicle-treated WT and Tg6799 mice (Fig. 3, B and C). Approximately half (52.7 ± 12.1%) of the vessels were occluded in vehicle-treated WT mice, but 95.6 ± 3.5% of vessels were occluded in vehicle-treated Tg6799 mice. RU-505 treatment significantly lowered the vessel occlusion in Tg6799 mice to 60.7 ± 8.7%, but did not change vessel occlusion in WT mice (54.2 ± 11.8%). These results suggest that our lead compound significantly restored altered thrombosis and fibrinolysis in AD mice without affecting normal thrombosis and fibrinolysis in WT littermates.

Treatment with RU-505 reduced vascular Aβ deposition

CAA has been implicated in vascular degeneration of AD (Chen et al., 2006; Okamoto et al., 2010). Our previous studies showed that the Aβ–fibrinogen interaction increases Aβ fibrillization (Ahn et al., 2010). Thus, we investigated whether treatment of Tg6799 mice with RU-505 for 4 mo could decrease Aβ deposition in blood vessels. Aβ deposits were stained using Congo red, and blood vessels were labeled using laminin (green; Fig. 4 A). We quantified CAA area in the cortex

Table 2. Workflow of high-throughput screening using a focused library

Step	Test compound concentration	Number of compounds	% of picked compounds	Inhibition cut-off
Library compound	-	2,092	-	-
AlphaLISA (AL) assay hits	5, 10, and 20 µM	327	15.6	Inhibition >35% at 5 µM and >50% at 10 µM
Filtering using quenching (AL)	10 µM	58	2.77	Quenching <27% at 10 µM and inhibition >55% at 10 µM
Lipinski's rule		50	2.39	≤1 violation
Validation/dose response hits (FP and AL)	0.01–20 µM	5	0.24	IC_{50} < 3 µM (FP) and <10 µM (AL)

Selection criteria and number of compounds selected during each step of screening.

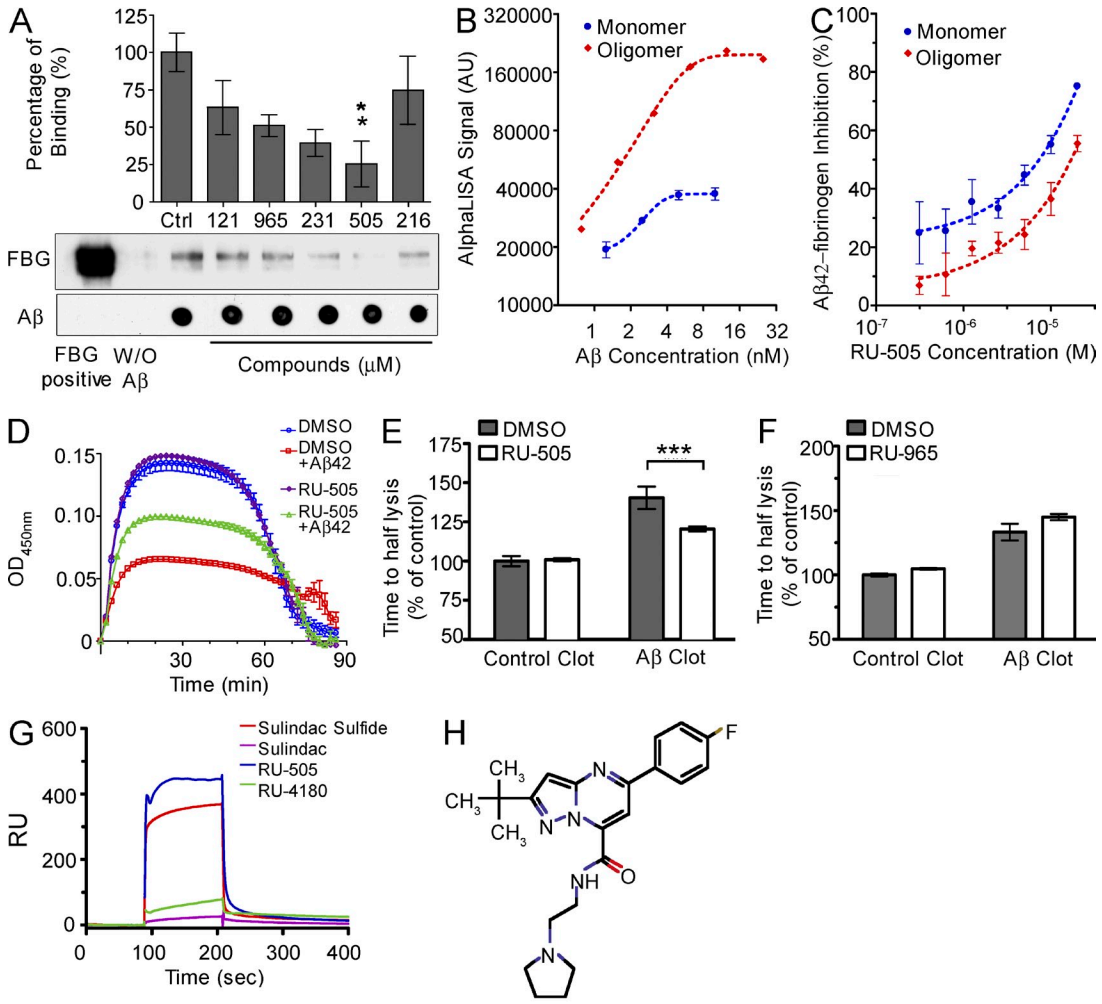

Figure 2. RU-505 inhibited the Aβ–fibrinogen interaction and restored Aβ-induced altered fibrin clot formation and degradation. (A) Candidate compounds (10 μM) were incubated with biotinylated Aβ42 and fibrinogen, and pull-down assays were performed using streptavidin–Sepharose. All samples were analyzed by Western blot. Dot blots were performed to control for amounts of Aβ pulled down. Control (Ctrl) lane contains only Aβ and fibrinogen without any compound (one-way ANOVA and Bonferroni post-hoc test; *, $P < 0.05$; $n = 3$–4 independent experiments). (B) The binding affinity between fibrinogen and monomeric or oligomeric biotinylated Aβ42 was measured using the AL assay. ($n = 3$–4 experiments, data are representative of three independent experiments). (C) The inhibitory efficacy of RU-505 on the interaction between fibrinogen and monomeric or oligomeric biotin-LC-Aβ42 was accessed in dose–response experiments using the AL assay. ($n = 3$–4 experiments, data are representative of three independent experiments). (D) RU-505 or DMSO was incubated with fibrinogen in the presence or absence of Aβ42, followed by plasminogen, thrombin, tPA, and $CaCl_2$. Fibrin clot formation was assessed by measuring turbidity ($n = 3$ experiments, data are representative of three independent experiments). (E and F) The time to fibrin clot degradation was analyzed by measuring time to half lysis. Control clot half lysis time was set to 100% for each experiment and all other values were calculated relative to controls. (***, $P < 0.001$; $n = 3$ experiments, data are representative of three independent experiments). (G and H) Aβ42 was immobilized on the SPR sensor chip surface, and the interaction of the indicated compounds with Aβ42 was analyzed using Biacore 3000. Sulindac sulfide (known to bind Aβ42) was a positive control, and sulindac was negative control. (H) Chemical structure of RU-4180. Data are representative of three to four independent experiments. All values are means and SEM.

by measuring Congo red deposits inside blood vessels, and Aβ plaque deposition was quantified by measuring Congo red outside blood vessels. The CAA area of RU-505–treated Tg6799 mice (0.025 ± 0.006%, cortex) was significantly decreased from that of vehicle-treated Tg6799 mice (0.046 ± 0.004%, cortex; Fig. 4 C). However, there was no significant difference in Aβ plaque area in the cortex between RU-505– and vehicle-treated Tg6799 mice (Fig. 4, B and D). WT mice did not exhibit any CAA-specific pattern of Congo red staining. This result indicates that inhibition of the Aβ–fibrinogen interaction by RU-505 reduced Aβ deposits in blood vessels of AD mice.

Treatment with RU-505 improved cognitive impairment of AD mice

Because RU-505 restored Aβ-induced altered thrombosis and impaired fibrinolysis in vitro and in vivo, we explored whether long-term RU-505 treatment could have behavioral

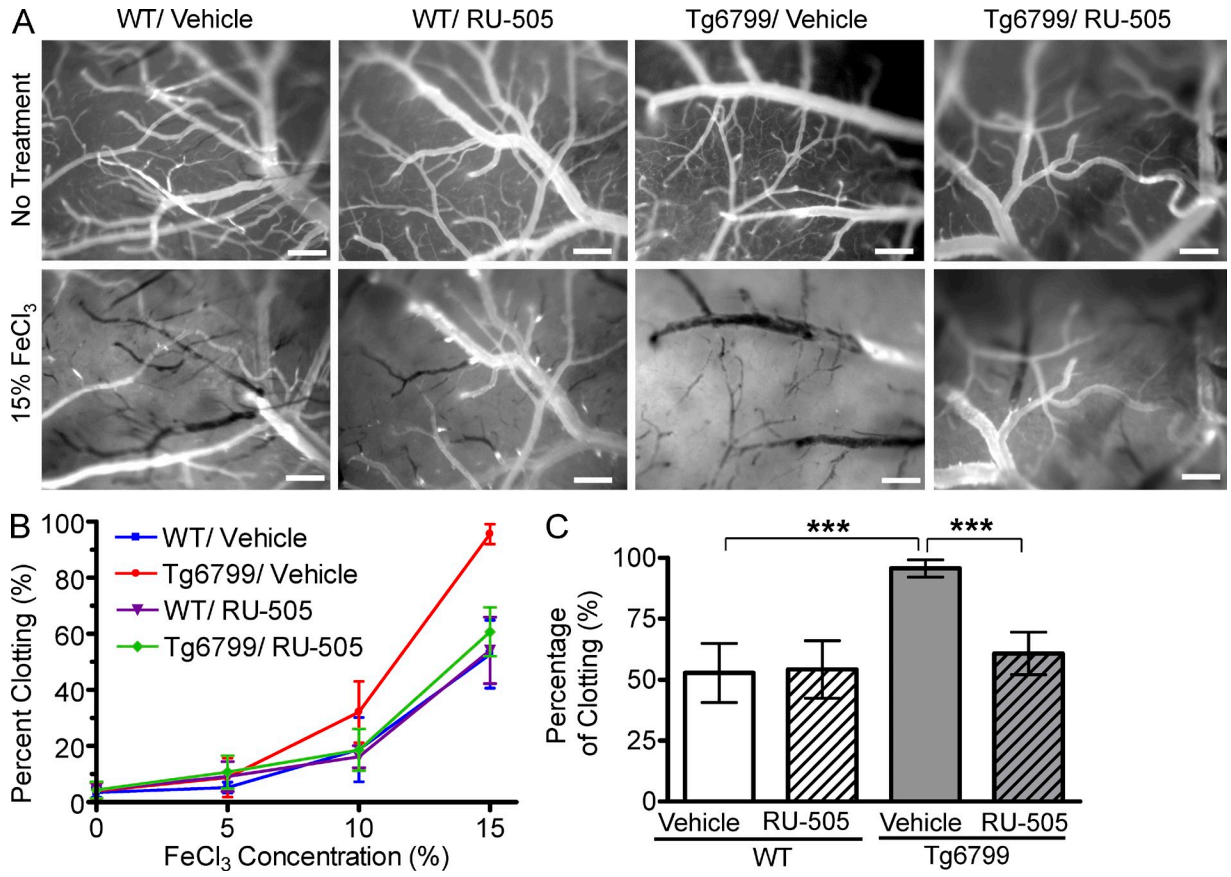

Figure 3. RU-505 prevented altered thrombosis and fibrinolysis in AD transgenic mice. (A) After craniotomy, three concentrations of $FeCl_3$ (5, 10, and 15%) were incrementally administered to the surface of the brains of vehicle- or RU-505–treated WT and Tg6799 mice (Videos 1–4), and clotting of cerebral blood vessels (>20 µM) was imaged (bars, 200 µm). Representative intravital images shows the surface of the brains of vehicle- or RU-505–treated WT and Tg6799 mice before $FeCl_3$ treatments or 5 min after 15% $FeCl_3$ treatments. (B and C) Frequency of clotted vessels was calculated at increasing concentrations of $FeCl_3$ (B) and was plotted for 15% $FeCl_3$ treatment (C; ***, $P < 0.001$; $n = 5$ mice per group). All values are means and SEM. Results are from two independent experiments.

effects on AD mice. 7-mo-old Tg6799 mice treated for 3 mo with RU-505 were tested using contextual fear conditioning to assess possible cognitive changes. RU-505 treatment had no effect on baseline freezing behavior in WT and Tg6799 mice (Fig. 5 A). When we evaluated contextual memory of Tg6799 and WT mice 24 h after training, vehicle-treated Tg6799 mice showed a severe memory deficit compared with vehicle-treated WT mice (Fig. 5 B). RU-505–treated Tg6799 mice exhibited significantly improved memory compared with their vehicle-treated AD counterparts, whereas long-term treatment of RU-505 in WT mice did not impact basal freezing behavior or contextual memory.

We also explored cognitive performance of RU-505–treated Tg6799 mice with the Barnes maze, a behavioral test that assesses spatial learning and memory in rodents (Walker et al., 2011). Vehicle-treated Tg6799 mice took a significantly longer amount of time to find the target hole compared with vehicle-treated WT and RU-505–treated Tg6799 mice (Fig. 5 C). During the memory retention test in the probe trials, vehicle-treated Tg6799 mice also had significantly longer latency to reach the closed target hole (Fig. 5 D) and significantly fewer visits to the target hole compared with vehicle-treated WT and RU-505–treated Tg6799 mice (Fig. 5 E). These results suggested that vehicle-treated Tg6799 mice have impaired spatial learning and memory, and RU-505 treatment restored the cognitive impairment of Tg6799 mice. When we measured total distance traveled during probe trials, Tg6799 mice moved significantly less than WT mice. However, there was no significant difference in distance traveled between RU-505–treated and untreated Tg6799 mice (Fig. 5 F). This result suggests that the better performance of RU-505–treated Tg6799 mice compared with untreated Tg6799 mice is likely caused by memory improvement and not effects on locomotion.

To further address any possible issue of hypoactivity in the Tg6799 mice and to test whether RU-505 treatment had a similar effect on a different strain of AD transgenic mice, we administered RU-505 to 4-mo-old TgCRND8 mice (Chishti et al., 2001) for 3 mo (analyzed at 7 mo-of-age) as a pilot experiment. During training, RU-505 treatment did not lead to

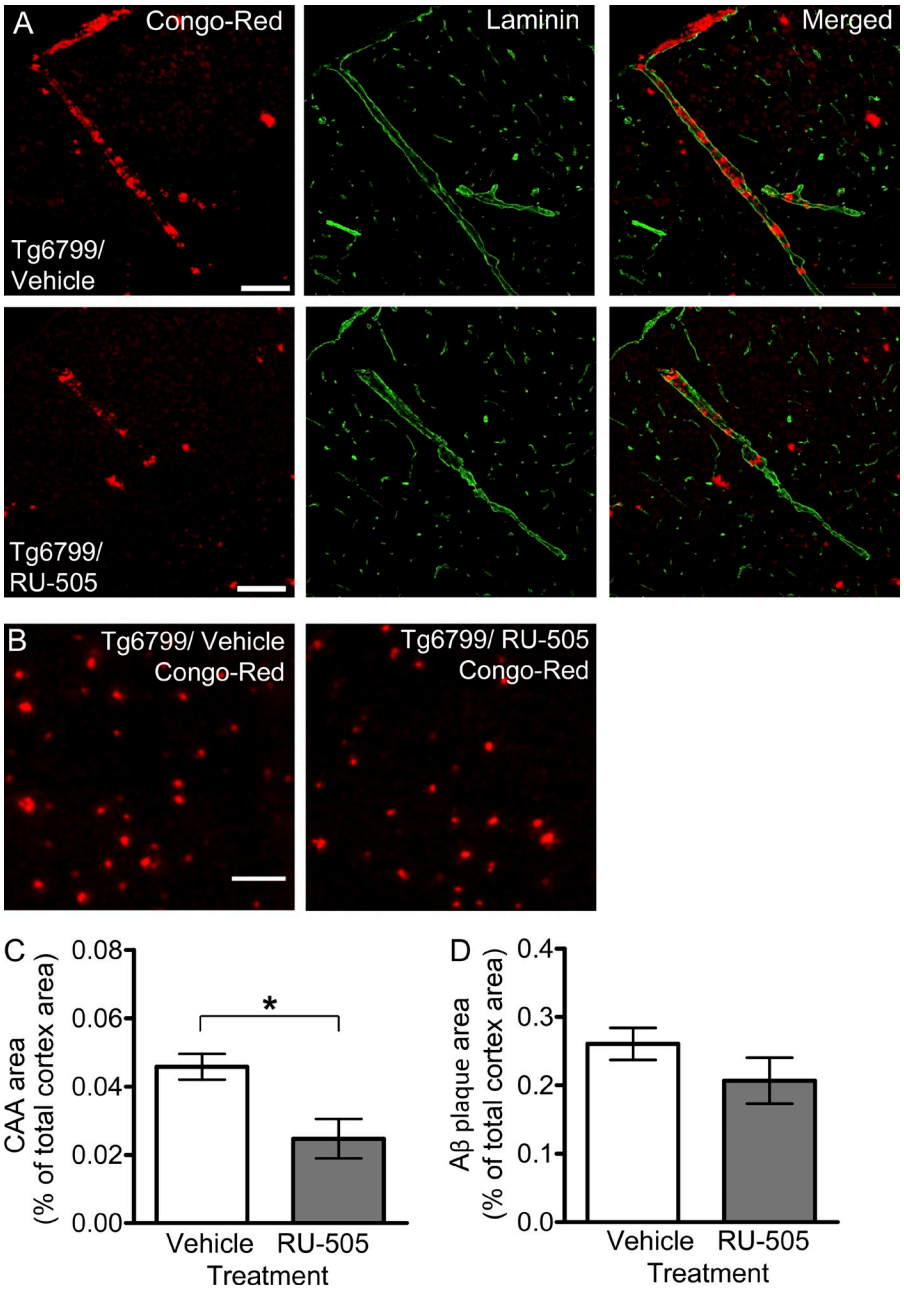

Figure 4. CAA pathology in AD transgenic mice was reduced after long-term treatment with RU-505. (A) Aβ deposits within cortical blood vessels of vehicle- or RU-505–treated Tg6799 mice were visualized using Congo red and laminin (green) labeling (bars, 100 µm). (B) Representative pictures showing parenchymal Aβ deposition in untreated and treated mice (bars, 100 µm). (C and D) CAA and Aβ plaques in (A) and (B) were quantified from 7–10 sections per mouse (n = 5 mice per group; *, $P < 0.05$). All values are means and SEM. Results are from two independent experiments.

improvement in spatial learning in TgCRND8 mice (Fig. 6 A); however, this treatment significantly reduced the latency to reach the target hole during the probe trial compared with vehicle-treated TgCRND8 mice (Fig. 6 B). Furthermore, the number of visits to the target hole during the probe trial was significantly higher in RU-505–treated TgCRND8 mice compared with vehicle-treated TgCRND8 mice (Fig. 6 C). In addition, vehicle-treated TgCRND8 mice showed similar locomotor activity during probe trials (Fig. 6 D), indicating that the impaired performance of vehicle-treated TgCRND8 mice in Barnes maze test is more likely caused by deficits in spatial memory. These results suggest that treatment of RU-505 substantially improved the deficits in spatial memory of TgCRND8 mice.

Long-term treatment with RU-505 decreased the level of infiltrated fibrinogen and microgliosis in AD mice

To understand the mechanisms underlying improvement in cognitive function of RU-505–treated AD mice, we analyzed cortical fibrinogen infiltration and microgliosis in Tg6799 mice after four months of RU-505 treatment. BBB permeability is increased in mouse models of AD (Paul et al., 2007) and infiltrated fibrinogen might bind to Aβ and become resistant to degradation in the parenchyma. If RU-505 can inhibit the interaction between infiltrated fibrinogen and Aβ in the parenchyma, the level of infiltrated fibrinogen could be decreased in the brain of AD mice. In addition, activation of microglia is highly increased

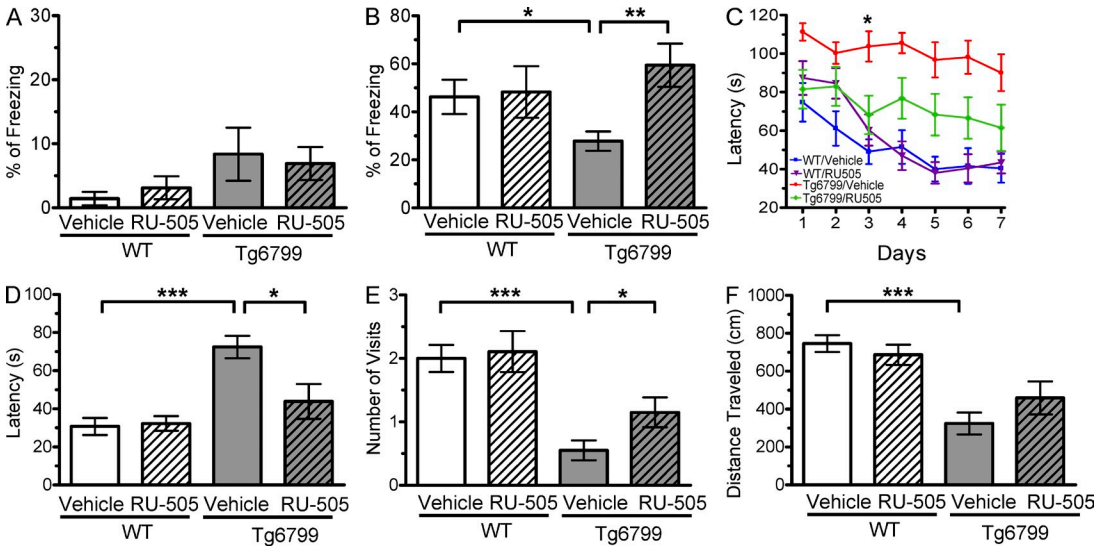

Figure 5. RU-505 restored cognitive function in Tg6799 mice. (A) Freezing behavior was measured before electric foot shock during the training day to assess the basal freezing tendency of each group of mice. (n = 8–10 mice per group). (B) Contextual memory was assessed by measuring freezing behavior upon reexposure to the training chamber 24 h after fear conditioning training. (*, $P < 0.05$; **, $P < 0.01$; n = 8–10 mice per group). Results are from two independent experiments. (C–E) Spatial learning and memory retention of WT and Tg6799 mice was assessed using the Barnes maze after 3 mo of treatment with RU-505 or vehicle. One target hole was connected to a hidden escape chamber. (C) During training trials, latency to poke the target hole was measured. Significance was assessed using two-way ANOVA analysis with repeated measure (WT/vehicle vs. Tg6799/vehicle: $F_{[1,120]} = 40.47$; $P < 0.001$; Tg6799/vehicle vs. Tg6799/RU-505: $F_{[1,108]} = 11.97$; $P < 0.01$; n = 10–14 mice per group). Differences in latency were assessed by Bonferroni post hoc analysis. (D–F) During the Barnes maze probe trial, latency to reach the closed target hole (D), number of visits to the target hole (E), and total traveled distance (F) were measured ([E] *, $P < 0.05$; **, $P < 0.01$; ***, $P < 0.001$; n = 10–14 mice per group; [F] ***, $P < 0.001$; n = 10–14 mice per group). All results of the Barnes maze are from three independent experiments.

in AD patients and mouse models of AD, and an increase of inflammation in the brain is correlated with memory impairment (Bayer et al., 1999; Dhawan and Combs, 2012; Vom Berg et al., 2012).

Therefore, we measured the level of infiltrated fibrinogen and microgliosis in the cortex of Tg6799 or WT littermate mice after RU-505 treatment. We quantified fibrinogen deposition (green; Fig. 7 A) outside the endothelial cells of blood vessels that were labeled using CD31 (red; Fig. 7 A), and the area of activated microglia that were labeled using CD11b (red; Fig. 7 B). The levels of infiltrated fibrinogen and microgliosis were highly increased in the cortex of Tg6799 compared with WT mice (Fig. 7, C and D), and these increases were significantly decreased by RU-505 (Fig. 7, C and D).

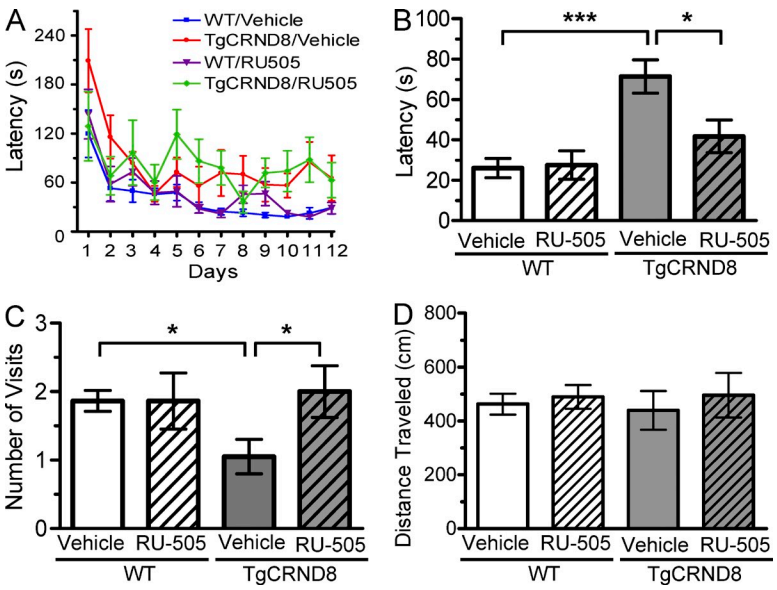

Figure 6. RU-505 restored spatial retention memory in TgCRND8 mice without affecting motor behavior. (A) The spatial memory of vehicle- or RU-505–treated WT and TgCRND8 mice was assessed using Barnes maze. (B and C) Spatial memory of RU-505–treated WT and TgCRND8 mice was tested using the Barnes maze probe trials. Time to reach the target hole (B), the number of visits to the closed target hole (C), and total distance traveled (D) were assessed (n = 7–11 mice per group). The results corroborate those in Fig. 5 and are from one experiment. All values are means and SEM.

DISCUSSION

The present study shows that the novel compound, RU-505, restored Aβ-induced altered thrombosis and delayed fibrinolysis in vitro and in vivo by inhibiting the Aβ–fibrinogen interaction. We also demonstrate that long-term RU-505 treatment can reduce vascular amyloid deposits, infiltrated fibrinogen, and microgliosis in the cortex of a transgenic mouse model of AD. Finally, this novel Aβ–fibrinogen interaction inhibitor improved the cognitive decline of two different strains of AD transgenic mice.

Using pharmacokinetics, we found that RU-505 is highly permeable to the BBB because RU-505 levels in the brain were equal to or greater to that in the blood over a 24-h period after single subcutaneous injection. The half-life of RU-505 was ∼3.7 h in the blood and ∼12.4 h in the brain. Therefore, the intravascular and the tunica media of arterioles are the most likely regions for RU-505 action. Several studies have shown that the amount of soluble Aβ significantly increases in the vicinity of amyloid deposits in blood vessels (Shinkai et al., 1995; Suzuki et al., 1994), and the intravascular area near CAA might be a major target of inhibition by RU-505. In addition, the increased infiltrated fibrinogen in AD mice may interact with Aβ in the tunica media of arterioles, which could be another target region for inhibition of Aβ-induced exacerbated thrombosis, as well as for prevention of CAA formation.

One question that arises from our results is why RU-505 treatment reduced vascular amyloid deposits, but not parenchymal plaque. Amyloid accumulates in the tunica media of arterioles in CAA, and the tunica media is much closer to the intravascular region than the parenchyma. Therefore, the fibrinogen levels in the tunica media should be much higher than in the parenchyma. For this reason, the Aβ–fibrinogen interaction could be a major factor of Aβ fibrillization in CAA, but have only minor effects on Aβ fibrillization on parenchymal plaques.

We primarily investigated the interaction between Aβ42 and fibrinogen in this study, but the ratio of Aβ40 to Aβ42 is higher in CAA. Another question is how RU-505, an inhibitor of the Aβ42–fibrinogen interaction, could reduce CAA, which is primarily composed of Aβ40. One possibility is that Aβ40 also interacts with fibrinogen even though its

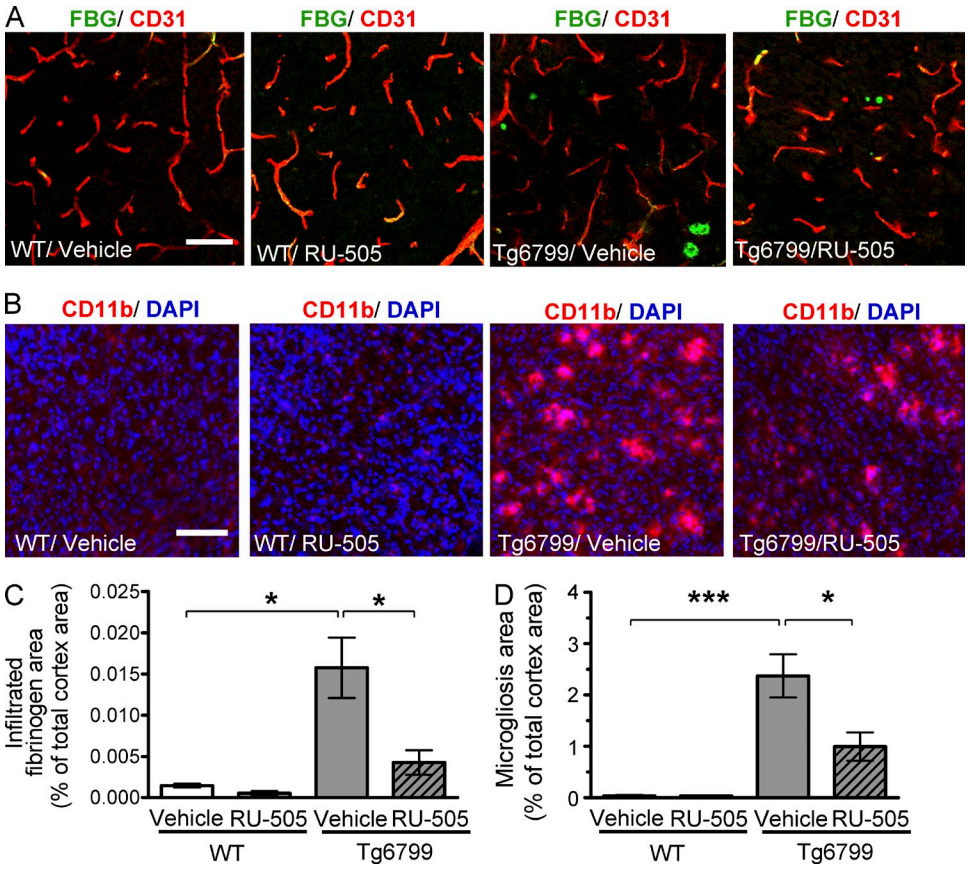

Figure 7. Long-term treatment with RU-505 reduced the level of infiltrated fibrinogen and microgliosis in the cortex of Tg6799 mice. (A) Fibrinogen localized outside of endothelial cells of blood vessels was labeled with FITC-conjugated antifibrinogen antibody (green), and endothelial cells were labeled using anti-CD31 antibody (red; bars, 50 µm). (B) Activated microglia were visualized by staining for CD11b (red). DAPI staining (blue) was used to show integrity of tissue (bars, 100 µm). (C and D) Total fibrinogen area (C) and microgliosis (D) were quantified from 3 sections per mouse (n = 3–4 mice per group; *, $P < 0.05$; ***, $P < 0.001$). All values are means and SEM. Results are from two independent experiments.

affinity is 10 times less than Aβ42, and RU-505 has a strong inhibitory efficacy on Aβ40–fibrinogen interaction (unpublished data). Therefore, RU-505 could reduce CAA through inhibition of both Aβ42- and Aβ40–fibrinogen interaction. Second, despite the higher levels of Aβ40 in vascular amyloid, Aβ42 is also essential for vascular amyloid deposition in transgenic mice overexpressing human APP (Van Dorpe et al., 2000; McGowan et al., 2005) and AD human patients (Roher et al., 1993; Shinkai et al., 1995). Aβ42 could act as a nucleation seed of amyloid deposit in the vessel walls and accelerate deposition of Aβ40 (Van Dorpe et al., 2000; Yoshiike et al., 2003; McGowan et al., 2005). Therefore, even though the ratio of Aβ40 to Aβ42 is higher in vascular amyloid, the Aβ42–fibrinogen interaction could be critically involved in CAA formation.

Fibrinogen is a proinflammatory mediator in several diseases and induces the activation of microglia in the nervous system (Adams et al., 2007; Davalos and Akassoglou, 2012). Our study showed that RU-505 treatment reduced the level of infiltrated fibrinogen and activated microglia in the brain of AD transgenic mice. One possible mechanism for this reduction is that RU-505 binds Aβ, inhibits the Aβ–fibrinogen interaction, and facilitates fibrinogen degradation. The decreased level of infiltrated fibrinogen could result in the decrease of microgliosis. The other possible mechanism is that long-term RU-505 treatment reduced vascular amyloid deposits and prevented BBB leakage. This recovery of a healthy BBB could reduce fibrinogen infiltration and inflammation in the parenchyma of Tg6799 mice.

Increased levels of plasma fibrinogen are associated with cognitive deficits (Xu et al., 2008), AD risk (van Oijen et al., 2005), and brain atrophy (Thambisetty et al., 2011), and increased levels of fibrinogen have also been found in the CSF of AD patients (Craig-Schapiro et al., 2011; Vafadar-Isfahani et al., 2012). Moreover, several studies have shown that anticoagulant treatment improves cognition in mouse models of AD and dementia patients (Ratner et al., 1972; Walsh et al., 1978; Cortes-Canteli et al., 2010; Timmer et al., 2010). However, anticoagulant therapy can cause severe problems in elderly patients who have a more fragile vasculature because it may increase the incidence of major systemic bleeding. Therefore, drugs should specifically block the Aβ–fibrinogen interaction so that Aβ-induced altered blood clot formation and degradation can be restored without affecting general hemostasis. RU-505 successfully targeted only Aβ-induced altered blood clot formation and did not affect general clot formation and degradation (Fig. 2 D and Fig. 3).

The maximum tolerated dose of RU-505 after single intravenous dose in mice was between 100 and 200 mg/kg. When we treated Tg6799 mice and WT littermates with two doses (100 and 50 mg/kg) of RU-505 every other day for 3 mo, we found that 100 mg/kg for long-term treatment was toxic to the AD mice, but 50 mg/kg showed no clinical signs of toxicity except local chronic inflammation at the injection site. To address the issue of local inflammation, we lowered the dose to 35 mg/kg for Tg6799 or 25 mg/kg for TgCRND8 over 3 mo, which minimized this issue. Our future direction would modify RU-505, and find less toxic analogues with similar or better efficacy.

For more than a decade, Aβ has been the major target for developing AD therapies. Most of these efforts focused on using antibodies to lower Aβ levels, preventing Aβ aggregation, or reducing Aβ production. However, none of these methods were successful as the treatments did not show clinical efficacy or caused serious adverse side effects such as aseptic meningoencephalitis (Gilman et al., 2005; Mangialasche et al., 2010). However, numerous studies still support the hypothesis that Aβ plays an important role in the pathogenesis of AD (Tanzi and Bertram, 2005; Jonsson et al., 2012). Therefore, new strategies for anti-Aβ therapy are necessary for developing novel treatments for AD. Inhibiting the interaction between Aβ and its binding proteins could be an alternative therapeutic approach, and our study shows that a small molecule, bioavailable inhibitor of the Aβ–fibrinogen interaction, RU-505, significantly restored altered thrombosis and improved cognitive deficits observed in AD transgenic mouse models. Therefore, treatment of the neurovascular pathology observed in AD using an inhibitor of the Aβ–fibrinogen interaction may be a valuable strategy for developing novel AD therapeutics.

MATERIALS AND METHODS

Animals

Tg6799 mice (The Jackson Laboratory) are double transgenic mice for APP/Presenilin 1 that coexpress five early onset familial AD mutations on a mixed background C57BL/6 x_SJL (Oakley et al., 2006). TgCRND8 mice (provided by A. Chishti and D. Westaway, University of Toronto, Canada) have three APP mutations (K670N, M671L, and V717F) driven by the human prion protein promoter on a mixed background C57 x C3H/C57 (Chishti et al., 2001). RU-505 was prepared in 2.5% EtOH, 4.5% Cremophor RH40 (Sigma-Aldrich), and 14% D5W (5% dextrose in water) in saline. We administered 35 mg/kg dose of RU-505 or vehicle to Tg6799 mice and 25 mg/kg dose or vehicle to TgCRND8 mice subcutaneously every other day. Nontransgenic (WT) littermates were used in all experiments. The assigned genotype of all the mice used in the experiments throughout the paper was double-checked by taking tail tissue the day of sacrifice. Only male mice were used in experiments, and all animals were maintained in The Rockefeller University Comparative Biosciences Center and treated in accordance with protocols approved by The Rockefeller University Institutional Animal Care and Use Committee.

Primary compound screening

Approximately 93,000 compounds were screened using HTS. Compound screening libraries that include known off-patent drugs, natural products, and combinatorially elaborated active pharmacophores were purchased from several vendors listed in Table 3. The primary assay used FP to measure the changes in the anisotropy induced by binding of TAMRA-labeled Aβ42 (Anaspec) to fibrinogen. TAMRA-Aβ42 (2 nM) was mixed with 300 nM fibrinogen (EMD Millipore) and 20 μM compounds (dissolved in 1% DMSO [final]) in 50 mM PBS, pH 7.4, 0.001% Tween 20, and 0.001% BSA as 50 μl final volume in black 384-well plates (Greiner) at RT. After binding reached equilibrium, polarization measurements were recorded with a Perkin-Elmer EnVision plate reader with excitation at 490 nm and emission at 535 nm. The FP response was monitored and plotted as milli-Polarization (mP) units.

Compounds that showed >75% inhibition of the Aβ–fibrinogen interaction in the FP assay were selected for screening by AlphaLISA as a secondary assay. Compounds (12.5 μM) were plated in white 384-well plates

(Greiner) and were incubated with 10 nM biotinylated Aβ42 (Anaspec) and 1 nM fibrinogen for 30 min at RT in final volume of 10 µl assay buffer (25 mM Tris-HCl, pH 7.4, 150 mM NaCl, 0.05% Tween-20, and 0.1% BSA). The mixture was incubated with anti–fibrinogen antibody (Dako), 20 µg/ml streptavidin-conjugated donor, and protein A–conjugated acceptor beads (PerkinElmer) for 90 min at RT. Samples were read by a PerkinElmer EnVision plate reader.

Hit compounds from the secondary assay were evaluated using Lipinski's Rule of Five to determine whether each chemical compound has properties that make it a potential usable drug. If compounds violated more than one of Lipinski's Rule of Five, those compounds were removed from our list. The AlphaScreen TruHits kit (PerkinElmer) was used to detect those compounds that react with singlet oxygen and thus unspecifically quench the assay. The AlphaScreen TruHits kit also allows for the identification of color quenchers, light scatterers (insoluble compounds), and biotin mimetics interfering with the AlphaLISA signal. If inhibition by quenching was more than 30% at 10 µM compound, those compounds were removed from our list. After completing the quenching test, we screened hit compounds in a dose–response experiment with various compound concentrations (0.01–20 µM) using FP and AlphaLISA. The data were fitted to sigmoidal dose–response equation ($Y = Bottom + (Top - Bottom)/1 + 10^{(logIC50 - X) \times Hill\ coefficient)}$) using GraphPad Prism 4 to calculate half-maximal inhibition (IC_{50}) of each compound. Compounds with $IC_{50} < 50$ µM in both FP and AlphaLISA were purchased as powder and were retested in dose–response experiments using both assays.

Analogue compound screening

To improve our candidate compounds, we had access to the ChemNavigator database, which has 50 million commercially available compounds and software for Tanimoto-based similarity searching. We purchased ∼2,000 analogue compounds through ChemNavigator or directly from Albany Molecular Research Inc. These analogues were tested using AlphaLISA at 5, 10, and 20 µM. We selected compounds which have >50% inhibition at 10 µM and a proportional inhibitory effect at 5 or 20 µM. Drug-like compounds were evaluated using Lipinski's Rule of Five, and false-positive compounds were filtered out using the AlphaScreen TruHits kit (PerkinElmer) as described above. Compounds with $IC_{50} < 10$ µM in both FP and AlphaLISA were selected using dose–response experiments. Selected compounds were purchased as powder and were retested in dose–response experiments using both assays. Finally, we identified hit compounds of with $IC_{50} < 3$ µM in FP and $IC_{50} < 10$ µM AlphaLISA assay.

Pull-down assay

Hit compounds were tested using a pull-down assay as described previously (Ahn et al., 2010). In brief, compounds at 10 µM were incubated with 100 nM biotinylated Aβ42 (Anaspec) and 5 nM fibrinogen (EMD Millipore) for 1 h at room temperature in 500 µl of binding buffer (50 mM Tris-HCl, pH 7.4, 150 mM NaCl, 0.1% Nonidet P-40, 0.1% BSA, and protease inhibitor mixture). The samples were gently rotated for 1 h at room temperature with 30 µl streptavidin–Sepharose high performance beads (GE Healthcare). After incubation, the beads were washed five times with binding buffer, and nonreducing sample buffer was added to the beads for elution. Western blots were performed using antifibrinogen antibody (Dako). Dot blots were performed using anti-Aβ antibody 4G8 (Covance) to show comparable amounts of Aβ were also being pulled down.

Table 3. Vendor list for primary screening library

Provider	No. of compound from each provider
ChemDiv	21,986
Prestwick	1,110
Cerep	4,000
ChemBridge	5,000
Microsource	2,000
AMRI	50,000
Biofocus	7,750
GreenPharma	240
Sigma LOPAC	1,280
Prof. Derek Tan (Memorial Sloan-Kettering Cancer Center, New York, NY)	350
Total	93,716

The binding assay between fibrinogen and monomeric or oligomeric Aβ42

Biotin-Aβ42 monomers and oligomers were prepared as in (Stine et al., 2011). In brief, biotin-LC-Aβ42 (Anaspec) was monomerized by treatment with hexafluoroisopropanol, dissolved to 5 mM with dimethyl sulfoxide, then diluted to 100 µM with cold PBS, and sonicated. Monomeric biotin-LC-Aβ42 was incubated at 4°C for 24 h for oligomeric preparation. 1 nM fibrinogen was mixed with increasing concentrations of monomeric or oligomeric biotin-LC-Aβ42 (0.5–20 nM) for 30 min at room temperature and the binding affinity was measured using AlphaLISA assay. The inhibitory efficacy of RU-505 on the interaction between fibrinogen and monomeric or oligomeric biotin-LC-Aβ42 was accessed in dose–response experiments using AlphaLISA assay.

In vitro thrombosis and fibrinolysis assay

To test whether hit compound have an effect on fibrin clot formation and lysis, 20 µM of each compound (dissolved in 0.4% DMSO [final]) or DMSO control was incubated with fibrinogen (1.5 µM) in the presence or absence of Aβ42 (3 µM) for 10 min and then mixed with plasminogen (0.25 µM) in 20 mM Hepes buffer (pH 7.4) with 137 mM NaCl. Fibrin clot formation and degradation was analyzed measuring turbidity right after adding thrombin (0.5 U/ml), tPA (0.15 nM), and $CaCl_2$ (5 mM) in a final volume of 150 µl. Assays were performed at RT in High Binding 96-well plates (Thermo Fisher Scientific) in triplicate and were measured at 450 nm using a Spectramax Plus384 reader (Molecular Devices).

SPR

SPR experiments were performed to test whether our lead compounds bind to Aβ42 as described previously (Richter et al., 2010). Biacore 3000 instrument and CM5 sensor chips (GE Healthcare) were used for this assay. Hexafluoroisopropanol-treated monomerized Aβ42 was immobilized to the sensor chip surface by amine coupling. Compounds were diluted to 40 µM from DMSO stock solutions in PBS as running buffer (final 2% DMSO) and injected for 2 min at a flow rate of 30 µl/min using the KINJECT command. After the dissociation phase the chip was rinsed with 20 mM HCl. Corresponding DMSO dilutions were used as a buffer blank, and a solvent correction assay was performed to correct the difference of DMSO response between empty reference surface and protein-immobilized surface. Sulindac sulfide and sulindac were used as positive control and negative controls, respectively (Richter et al., 2010).

In vivo toxicity study

Maximum tolerated dose studies were performed to determine the toxicity of RU-505 (AMRI) and to identify the optimal dose for in vivo assays. Single injection toxicity was performed at Absorption Systems LP (Exton, PA), and four different doses (200, 100, 50, and 20 mg/kg mouse) of RU-505, along with saline and vehicle, were injected into male and female CD-1 mice intravenously. Mortality and overt clinical signs of toxicity were monitored for 2 d. All animals dosed with 200 mg/kg were found dead after single intravenous injection, and no clinical signs of toxicity were observed after single dose of 20, 50, or 100 mg/kg for 2 d after injection. Therefore, the maximum tolerated dose of RU-505 after single intravenous dose in mice was established as 100 mg/kg.

Because AD treatment would be long-term and toxicity of long-term treatment can be different from toxicity after a single injection, we treated Tg6799 mice and WT littermates with two doses (100 and 50 mg/kg) of RU-505 every other day for 3 mo, and overt clinical signs of toxicity were monitored. After 3 mo, mice were sent to the Laboratory of Comparative Pathology at Memorial Sloan-Kettering Cancer Center for complete necropsy and hematology reports to determine the effects of our lead compound after long-term treatment.

Pharmacokinetics

The pharmacokinetics of and BBB permeability to RU-505 were determined by assessing the drug's decay in blood plasma and brain homogenates over a 24-h period after subcutaneous injection (35 mg/kg) into WT mice of the same genetic background as Tg6799. Blood was collected in heparinized tubes after cardiac puncture 0.5, 1, 2, 4, 6, and 24 h after RU-505 administration. After perfusion, brains were collected and homogenized with PBS. Plasma and brain homogenates were sent to Apredica and were analyzed by LC/MS/MS using an Agilent 6410 mass spectrometer coupled with an Agilent 1200 HPLC. This analysis revealed that RU-505 penetrates the blood brain barrier, and RU-505 levels in the brain were equal to or greater than in the blood (~3 μM).

In vivo thrombosis assay

To observe blood circulation and to induce thrombosis, a cranial window was prepared as described previously (Cortes-Canteli et al., 2010). In brief, a cranial window was prepared over the parietal cortex of 7-mo-old Tg6799 mice and WT littermates which were treated with RU-505 (35 mg/kg) or vehicle for three months (n = 5 per group). Mice were anesthetized by i.p. injection of 500 mg/kg tribromethanol and 0.04 mg/kg atropine and placed in a custom built restraint system. A 2.5-mm circular craniotomy was prepared using 5–10 circular brush strokes with a fine dental drill bit, and a 4-mm plastic ring surrounding the window was attached with dental acrylic and cyanoacrylate adhesive. Sterile saline was applied periodically to protect the brain surface and prevent drying. For imaging of blood flow, 100 μl of 5 mg/ml 2 MDa FITC-conjugated dextran (Sigma-Aldrich) dissolved in PBS was administered by retroorbital injection. During the entire imaging session, the body temperature of mice was kept at 37.5°C using a TC-1000 Mouse complete temperature control system (CWE Inc.).

Increasing concentrations of $FeCl_3$ (5, 10, and 15%) were added directly to the brain surface with an interval of 5 min, and thrombosis was recorded using Olympus IX71 microscope equipped with Hamamatsu Orca ER B/W digital camera. MetaMorph acquisition software and 5× objective lens (NA = 0.25) were used for image collection. The total length of vessels with a >20 μm diam before $FeCl_3$ treatment and the total length of occluded vessels at 5 min after each $FeCl_3$ treatment (5, 10, and 15%) were measured. All analysis was performed using National Institutes of Health ImageJ software with the analyzer blinded to genotype and treatment of mice.

Immunohistochemistry for CAA and Aβ plaques

Mice were saline/heparin-perfused, and 20-μm coronal brain cryostat sections were fixed with 4% paraformaldehyde. Brain sections were incubated with rabbit anti–laminin antibody (Sigma-Aldrich) overnight and stained for 30 min with 0.2% Congo Red (Sigma) in 70% isopropanol. After immunohistochemistry, brain sections were analyzed with a microscope (Axiovert 200; Carl Zeiss) equipped with Plan-Neofluar (10× NA 0.3, and 20× NA 0.5) objective lenses at room temperature. The imaging medium was air for both the objective lenses used. The AxioCam color camera (Carl Zeiss) and AxioVision software (Carl Zeiss) were used for image collection. Each set of stained sections was processed under identical gain and laser power setting and under identical brightness and contrast settings. Images of all the areas with CAA and Aβ plaques were acquired and thresholded using Image J. The total area of CAA and Aβ plaques was analyzed as percentage of total cortex area with the analyzer blinded to treatment of mice. The average of 7–10 different sections from each mouse was determined (n = 5 mice per group).

Immunohistochemistry for infiltrated fibrinogen and microgliosis

Mice were saline/heparin-perfused, and 20 μm coronal brain cryostat sections were fixed with 50% methanol and 50% acetone. For fibrinogen and endothelial cell staining, brain sections were incubated with FITC-conjugated antifibrinogen antibody (Dako) and anti-CD31 antibody (BD) overnight. For activated microglia staining, brain sections were incubated with anti-CD11b antibody (DSHB) overnight. After immunohistochemistry, brain sections were analyzed with a confocal microscope (Inverted DMI 6000; Leica) equipped with HyD detectors and HCX PL APO CS (10× NA 0.4 and 20× NA 0.7) objective lenses at room temperature. The imaging medium was air for both the objective lenses used and Leica Application Suite Advanced Fluorescence was used for image collection as software. Each set of stained sections was processed under identical gain and laser power setting and under identical brightness and contrast settings. Images of brain section were acquired and thresholded using ImageJ. The total area of infiltrated fibrinogen or activated microglia was analyzed as percentage of total cortex area with the analyzer blinded to treatment of mice. The average of 3 different sections from each mouse was determined (n = 3–4 mice per group).

Behavioral analysis

All behavioral experiments were performed and analyzed with a researcher blinded to genotype and treatment. We administered 35 mg/kg of RU-505 or vehicle to 4-mo-old Tg6799 mice and WT littermates and 25 mg/kg or vehicle to 4-mo-old TgCRND8 mice and WT littermates subcutaneously every other day for three months (analyzed at 7 mo of age). Mice were handled and allowed to acclimate to the testing room for 10 min per day for at least 5 d.

Contextual fear conditioning

During training, Tg6799 mice and WT littermates (n = 8–10 per group) were allowed to explore the training chamber (Med Associates, Inc.) for the first 2 min, and then received three mild footshocks (2 s, 0.7 mA) spaced 1 min apart. Mice were removed from the training chamber 30 s after the last foot shock. Contextual learning was assessed 24 h after training by reexposing mice to the same training chamber for 3 min. Mouse behavior during training and testing was recorded, and freezing behavior was measured by observing mice every 5 s.

Barnes maze

The Barnes maze apparatus (TAP Plastics) consisted of a white circular platform (92 cm diam) with 20 equally spaced holes (5 cm in diameter; 7.5 cm between holes). Among these holes, one hole (target hole) was connected to a hidden black escape chamber. Bright lights (600 lx) were used to motivate the mice to find the target hole and enter into the escape chamber. Visual clues surrounded the maze. To remove any lingering scent on the maze from the previous animal, the platform and escape box were cleaned using 50% ethanol between mice. The entire experiment was recorded and analyzed using the Ethovision video tracking system (Noldus).

Tg6799 mice. Training consisted of two training trials per day over a period of 7 d (n = 10–14 per group). During each trial, mice were placed in the center of the maze in a black starting box for 30 s. After 30 s, the box was removed, and mice were allowed to freely explore and find the target hole within 2 min. Latency to poke the target hole was recorded. If mice did not enter into the escape chamber within 2 min, they were gently guided into the escape chamber and placed in the chamber for 30 s. To assess memory retention, a probe trial was conducted 24 h and 3 d after the last training. The target hole was closed like the other 19 holes, and the escape chamber was removed. Holes were kept in the same position as during the training. Mice were placed in the center of the maze in a black starting box for 30 s. After 30 s, the box was removed, and mice were allowed to freely explore for 90 s. The number of visits into each hole and the latency to reach the target hole were recorded. For analysis, scores of each mouse from both probe trials were combined and averaged.

TgCRND8 mice. Training consisted of a trial per day over a period of 12 d (n = 7–11 per group). During training, mice were placed in the center of the maze in a black starting box for 30 s. After 30 s, the box was removed, and mice were allowed to freely explore and find the target hole for 5 min. To assess memory retention, probe trials were conducted 24 h and 6 d after the last training. Mice were allowed to freely explore for 2 min during probe trials. The number of visits into each hole and the latency to reach the target hole were recorded. For analysis, scores of each mouse from both probe trials were combined and averaged.

Statistical analysis

All numerical values presented in graphs are mean ± SEM. Statistical significance of most experiments was determined using two-tailed t test analysis comparing control and experimental groups. The pull-down assay (Fig. 2 A) was analyzed using one-way ANOVA and Bonferroni post hoc test. Comparison of training curves from the Barnes maze (Fig. 5 C and Fig. 6 A) was analyzed using two-way ANOVA with repeated measure and Bonferroni post hoc test.

Online supplemental material

Video S1–S4 show intravital visualization of blood flow and blood vessel occlusion in Tg6799 mice or WT littermates that were treated with RU-505 or vehicle as increasing concentrations of $FeCl_3$ (5%, 10%, and 15%) were added directly to the brain surface. Online supplemental material are available at http://www.jem.org/cgi/content/full/jem.20131751/DC1.

The authors thank The Rockefeller University Bio-Imaging Resource Center for technical assistance, as well as Dr. Marta Cortes-Canteli, Dr. Zu-Lin Chen, and members of the Strickland Laboratory for discussion.

This work was supported by the Thome Memorial Medical Foundation, Alzheimer's Drug Discovery Foundation, National Institutes of Health (NS50537), Woodbourne Foundation, Mellam Family Foundation, May and Samuel Rudin Family Foundation, and the Blanchette Hooker Rockefeller Fund.

The authors have no conflicting financial interests.

Submitted: 20 August 2013
Accepted: 27 March 2014

REFERENCES

Adams, R.A., J. Bauer, M.J. Flick, S.L. Sikorski, T. Nuriel, H. Lassmann, J.L. Degen, and K. Akassoglou. 2007. The fibrin-derived gamma377-395 peptide inhibits microglia activation and suppresses relapsing paralysis in central nervous system autoimmune disease. *J. Exp. Med.* 204:571–582. http://dx.doi.org/10.1084/jem.20061931

Ahn, H.J., D. Zamolodchikov, M. Cortes-Canteli, E.H. Norris, J.F. Glickman, and S. Strickland. 2010. Alzheimer's disease peptide beta-amyloid interacts with fibrinogen and induces its oligomerization. *Proc. Natl. Acad. Sci. USA.* 107:21812–21817. http://dx.doi.org/10.1073/pnas.1010373107

Bayer, T.A., R. Buslei, L. Havas, and P. Falkai. 1999. Evidence for activation of microglia in patients with psychiatric illnesses. *Neurosci. Lett.* 271:126–128. http://dx.doi.org/10.1016/S0304-3940(99)00545-5

Brundel, M., J. de Bresser, J.J. van Dillen, L.J. Kappelle, and G.J. Biessels. 2012. Cerebral microinfarcts: a systematic review of neuropathological studies. *J. Cereb. Blood Flow Metab.* 32:425–436. http://dx.doi.org/10.1038/jcbfm.2011.200

Chen, Y.W., M.E. Gurol, J. Rosand, A. Viswanathan, S.M. Rakich, T.R. Groover, S.M. Greenberg, and E.E. Smith. 2006. Progression of white matter lesions and hemorrhages in cerebral amyloid angiopathy. *Neurology.* 67:83–87. http://dx.doi.org/10.1212/01.wnl.0000223613.57229.24

Chishti, M.A., D.S. Yang, C. Janus, A.L. Phinney, P. Horne, J. Pearson, R. Strome, N. Zuker, J. Loukides, J. French, et al. 2001. Early-onset amyloid deposition and cognitive deficits in transgenic mice expressing a double mutant form of amyloid precursor protein 695. *J. Biol. Chem.* 276:21562–21570. http://dx.doi.org/10.1074/jbc.M100710200

Cleary, J.P., D.M. Walsh, J.J. Hofmeister, G.M. Shankar, M.A. Kuskowski, D.J. Selkoe, and K.H. Ashe. 2005. Natural oligomers of the amyloid-beta protein specifically disrupt cognitive function. *Nat. Neurosci.* 8:79–84. http://dx.doi.org/10.1038/nn1372

Cortes-Canteli, M., J. Paul, E.H. Norris, R. Bronstein, H.J. Ahn, D. Zamolodchikov, S. Bhuvanendran, K.M. Fenz, and S. Strickland. 2010. Fibrinogen and beta-amyloid association alters thrombosis and fibrinolysis: a possible contributing factor to Alzheimer's disease. *Neuron.* 66:695–709. http://dx.doi.org/10.1016/j.neuron.2010.05.014

Craig-Schapiro, R., M. Kuhn, C. Xiong, E.H. Pickering, J. Liu, T.P. Misko, R.J. Perrin, K.R. Bales, H. Soares, A.M. Fagan, and D.M. Holtzman. 2011. Multiplexed immunoassay panel identifies novel CSF biomarkers for Alzheimer's disease diagnosis and prognosis. *PLoS ONE.* 6:e18850. http://dx.doi.org/10.1371/journal.pone.0018850

Davalos, D., and K. Akassoglou. 2012. Fibrinogen as a key regulator of inflammation in disease. *Semin. Immunopathol.* 34:43–62. http://dx.doi.org/10.1007/s00281-011-0290-8

de la Torre, J.C. 2004. Is Alzheimer's disease a neurodegenerative or a vascular disorder? Data, dogma, and dialectics. *Lancet Neurol.* 3:184–190. http://dx.doi.org/10.1016/S1474-4422(04)00683-0

Dhawan, G., and C.K. Combs. 2012. Inhibition of Src kinase activity attenuates amyloid associated microgliosis in a murine model of Alzheimer's disease. *J. Neuroinflammation.* 9:117. http://dx.doi.org/10.1186/1742-2094-9-117

Gilman, S., M. Koller, R.S. Black, L. Jenkins, S.G. Griffith, N.C. Fox, L. Eisner, L. Kirby, M.B. Rovira, F. Forette, and J.M. Orgogozo; AN1792(QS-21)-201 Study Team. 2005. Clinical effects of Abeta immunization (AN1792) in patients with AD in an interrupted trial. *Neurology.* 64:1553–1562. http://dx.doi.org/10.1212/01.WNL.0000159740.16984.3C

Jonsson, T., J.K. Atwal, S. Steinberg, J. Snaedal, P.V. Jonsson, S. Bjornsson, H. Stefansson, P. Sulem, D. Gudbjartsson, J. Maloney, et al. 2012. A mutation in APP protects against Alzheimer's disease and age-related cognitive decline. *Nature.* 488:96–99. http://dx.doi.org/10.1038/nature11283

Klohs, J., C. Baltes, F. Princz-Kranz, D. Ratering, R.M. Nitsch, I. Knuesel, and M. Rudin. 2012. Contrast-enhanced magnetic resonance microangiography reveals remodeling of the cerebral microvasculature in transgenic ArcAβ mice. *J. Neurosci.* 32:1705–1713. http://dx.doi.org/10.1523/JNEUROSCI.5626-11.2012

Lipinski, C.A., F. Lombardo, B.W. Dominy, and P.J. Feeney. 2001. Experimental and computational approaches to estimate solubility and permeability in drug discovery and development settings. *Adv. Drug Deliv. Rev.* 46:3–26. http://dx.doi.org/10.1016/S0169-409X(00)00129-0

Mangialasche, F., A. Solomon, B. Winblad, P. Mecocci, and M. Kivipelto. 2010. Alzheimer's disease: clinical trials and drug development. *Lancet Neurol.* 9:702–716. http://dx.doi.org/10.1016/S1474-4422(10)70119-8

McGowan, E., F. Pickford, J. Kim, L. Onstead, J. Eriksen, C. Yu, L. Skipper, M.P. Murphy, J. Beard, P. Das, et al. 2005. Abeta42 is essential for parenchymal and vascular amyloid deposition in mice. *Neuron.* 47:191–199. http://dx.doi.org/10.1016/j.neuron.2005.06.030

Mortimer, J.A. 2012. The Nun Study: risk factors for pathology and clinical-pathologic correlations. *Curr. Alzheimer Res.* 9:621–627. http://dx.doi.org/10.2174/156720512801322546

Neuropathology Group. Medical Research Council Cognitive Function and Aging Study; Neuropathology Group of the Medical Research Council Cognitive Function and Ageing Study (MRC CFAS). 2001. Pathological correlates of late-onset dementia in a multicentre, community-based population in England and Wales. *Lancet.* 357:169–175. http://dx.doi.org/10.1016/S0140-6736(00)03589-3

Oakley, H., S.L. Cole, S. Logan, E. Maus, P. Shao, J. Craft, A. Guillozet-Bongaarts, M. Ohno, J. Disterhoft, L. Van Eldik, et al. 2006. Intraneuronal beta-amyloid aggregates, neurodegeneration, and neuron loss in transgenic mice with five familial Alzheimer's disease mutations: potential factors in amyloid plaque formation. *J. Neurosci.* 26:10129–10140. http://dx.doi.org/10.1523/JNEUROSCI.1202-06.2006

Okamoto, Y., M. Ihara, H. Tomimoto, W. Taylor Kimberly, and S.M. Greenberg. 2010. Silent ischemic infarcts are associated with hemorrhage burden in cerebral amyloid angiopathy. *Neurology.* 74:93, author reply :93. http://dx.doi.org/10.1212/WNL.0b013e3181c77627

Park, L., J. Zhou, P. Zhou, R. Pistick, S. El Jamal, L. Younkin, J. Pierce, A. Arreguin, J. Anrather, S.G. Younkin, et al. 2013. Innate immunity receptor CD36 promotes cerebral amyloid angiopathy. *Proc. Natl. Acad. Sci. USA.* 110:3089–3094. http://dx.doi.org/10.1073/pnas.1300021110

Paul, J., S. Strickland, and J.P. Melchor. 2007. Fibrin deposition accelerates neurovascular damage and neuroinflammation in mouse models of Alzheimer's disease. *J. Exp. Med.* 204:1999–2008. http://dx.doi.org/10.1084/jem.20070304

Pfeifer, L.A., L.R. White, G.W. Ross, H. Petrovitch, and L.J. Launer. 2002. Cerebral amyloid angiopathy and cognitive function: the HAAS autopsy study. *Neurology*. 58:1629–1634. http://dx.doi.org/10.1212/WNL.58.11.1629

Ratner, J., G. Rosenberg, V.A. Kral, and F. Engelsmann. 1972. Anticoagulant therapy for senile dementia. *J. Am. Geriatr. Soc.* 20:556–559.

Richter, L., L.M. Munter, J. Ness, P.W. Hildebrand, M. Dasari, S. Unterreitmeier, B. Bulic, M. Beyermann, R. Gust, B. Reif, et al. 2010. Amyloid beta 42 peptide (Abeta42)-lowering compounds directly bind to Abeta and interfere with amyloid precursor protein (APP) transmembrane dimerization. *Proc. Natl. Acad. Sci. USA*. 107:14597–14602. http://dx.doi.org/10.1073/pnas.1003026107

Roher, A.E., J.D. Lowenson, S. Clarke, A.S. Woods, R.J. Cotter, E. Gowing, and M.J. Ball. 1993. beta-Amyloid-(1-42) is a major component of cerebrovascular amyloid deposits: implications for the pathology of Alzheimer disease. *Proc. Natl. Acad. Sci. USA*. 90:10836–10840. http://dx.doi.org/10.1073/pnas.90.22.10836

Ryu, J.K., and J.G. McLarnon. 2009. A leaky blood-brain barrier, fibrinogen infiltration and microglial reactivity in inflamed Alzheimer's disease brain. *J. Cell. Mol. Med.* 13(9A):2911–2925. http://dx.doi.org/10.1111/j.1582-4934.2008.00434.x

Shinkai, Y., M. Yoshimura, Y. Ito, A. Odaka, N. Suzuki, K. Yanagisawa, and Y. Ihara. 1995. Amyloid beta-proteins 1-40 and 1-42(43) in the soluble fraction of extra- and intracranial blood vessels. *Ann. Neurol.* 38:421–428. http://dx.doi.org/10.1002/ana.410380312

Smith, E.E., and S.M. Greenberg. 2009. Beta-amyloid, blood vessels, and brain function. *Stroke*. 40:2601–2606. http://dx.doi.org/10.1161/STROKEAHA.108.536839

Snowdon, D.A., L.H. Greiner, J.A. Mortimer, K.P. Riley, P.A. Greiner, and W.R. Markesbery. 1997. Brain infarction and the clinical expression of Alzheimer disease. The Nun Study. *JAMA*. 277:813–817. http://dx.doi.org/10.1001/jama.1997.03540340047031

Stine, W.B., L. Jungbauer, C. Yu, and M.J. LaDu. 2011. Preparing synthetic Aβ in different aggregation states. *Methods Mol. Biol.* 670:13–32. http://dx.doi.org/10.1007/978-1-60761-744-0_2

Suzuki, N., T. Iwatsubo, A. Odaka, Y. Ishibashi, C. Kitada, and Y. Ihara. 1994. High tissue content of soluble beta 1-40 is linked to cerebral amyloid angiopathy. *Am. J. Pathol.* 145:452–460.

Tanzi, R.E., and L. Bertram. 2005. Twenty years of the Alzheimer's disease amyloid hypothesis: a genetic perspective. *Cell*. 120:545–555. http://dx.doi.org/10.1016/j.cell.2005.02.008

Thal, D.R., W.S. Griffin, R.A. deVos, and E. Ghebremedhin. 2008. Cerebral amyloid angiopathy and its relationship to Alzheimer's disease. *Acta Neuropathol.* 115:599–609. http://dx.doi.org/10.1007/s00401-008-0366-2

Thambisetty, M., A. Simmons, A. Hye, J. Campbell, E. Westman, Y. Zhang, L.O. Wahlund, A. Kinsey, M. Causevic, R. Killick, et al; AddNeuroMed Consortium. 2011. Plasma biomarkers of brain atrophy in Alzheimer's disease. *PLoS ONE*. 6:e28527. http://dx.doi.org/10.1371/journal.pone.0028527

Timmer, N.M., L. van Dijk, C.E. van der Zee, A. Kiliaan, R.M. de Waal, and M.M. Verbeek. 2010. Enoxaparin treatment administered at both early and late stages of amyloid β deposition improves cognition of APPswe/PS1dE9 mice with differential effects on brain Aβ levels. *Neurobiol. Dis.* 40:340–347. http://dx.doi.org/10.1016/j.nbd.2010.06.008

Vafadar-Isfahani, B., G. Ball, C. Coveney, C. Lemetre, D. Boocock, L. Minthon, O. Hansson, A.K. Miles, S.M. Janciauskiene, D. Warden, et al. 2012. Identification of SPARC-like 1 protein as part of a biomarker panel for Alzheimer's disease in cerebrospinal fluid. *J. Alzheimers Dis.* 28:625–636.

Van Dorpe, J., L. Smeijers, I. Dewachter, D. Nuyens, K. Spittaels, C. Van Den Haute, M. Mercken, D. Moechars, I. Laenen, C. Kuiperi, et al. 2000. Prominent cerebral amyloid angiopathy in transgenic mice overexpressing the london mutant of human APP in neurons. *Am. J. Pathol.* 157:1283–1298. http://dx.doi.org/10.1016/S0002-9440(10)64644-5

van Oijen, M., J.C. Witteman, A. Hofman, P.J. Koudstaal, and M.M. Breteler. 2005. Fibrinogen is associated with an increased risk of Alzheimer disease and vascular dementia. *Stroke*. 36:2637–2641. http://dx.doi.org/10.1161/01.STR.0000189721.31432.26

Viswanathan, A., W.A. Rocca, and C. Tzourio. 2009. Vascular risk factors and dementia: how to move forward? *Neurology*. 72:368–374. http://dx.doi.org/10.1212/01.wnl.0000341271.90478.8e

Vom Berg, J., S. Prokop, K.R. Miller, J. Obst, R.E. Kälin, I. Lopategui-Cabezas, A. Wegner, F. Mair, C.G. Schipke, O. Peters, et al. 2012. Inhibition of IL-12/IL-23 signaling reduces Alzheimer's disease-like pathology and cognitive decline. *Nat. Med.* 18:1812–1819. http://dx.doi.org/10.1038/nm.2965

Walker, J.M., S.W. Fowler, D.K. Miller, A.Y. Sun, G.A. Weisman, W.G. Wood, G.Y. Sun, A. Simonyi, and T.R. Schachtman. 2011. Spatial learning and memory impairment and increased locomotion in a transgenic amyloid precursor protein mouse model of Alzheimer's disease. *Behav. Brain Res.* 222:169–175. http://dx.doi.org/10.1016/j.bbr.2011.03.049

Walsh, A.C., B.H. Walsh, and C. Melaney. 1978. Senile-presenile dementia: follow-up data on an effective psychotherapy-anticoagulant regimen. *J. Am. Geriatr. Soc.* 26:467–470.

Xu, G., H. Zhang, S. Zhang, X. Fan, and X. Liu. 2008. Plasma fibrinogen is associated with cognitive decline and risk for dementia in patients with mild cognitive impairment. *Int. J. Clin. Pract.* 62:1070–1075. http://dx.doi.org/10.1111/j.1742-1241.2007.01268.x

Yoshiike, Y., D.H. Chui, T. Akagi, N. Tanaka, and A. Takashima. 2003. Specific compositions of amyloid-beta peptides as the determinant of toxic beta-aggregation. *J. Biol. Chem.* 278:23648–23655. http://dx.doi.org/10.1074/jbc.M212785200

Zamolodchikov, D., and S. Strickland. 2012. Aβ delays fibrin clot lysis by altering fibrin structure and attenuating plasminogen binding to fibrin. *Blood*. 119:3342–3351. http://dx.doi.org/10.1182/blood-2011-11-389668